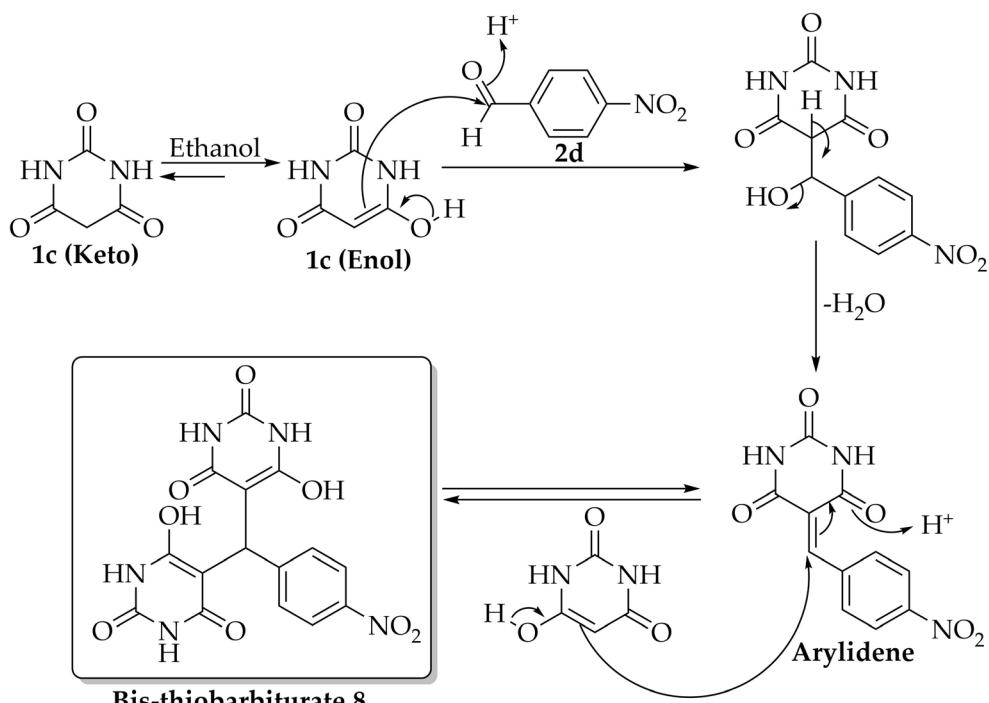


Supplementary Information

**Bis-thiobarbiturates as Promising Xanthine Oxidase Inhibitors:
Synthesis and Biological Evaluation**

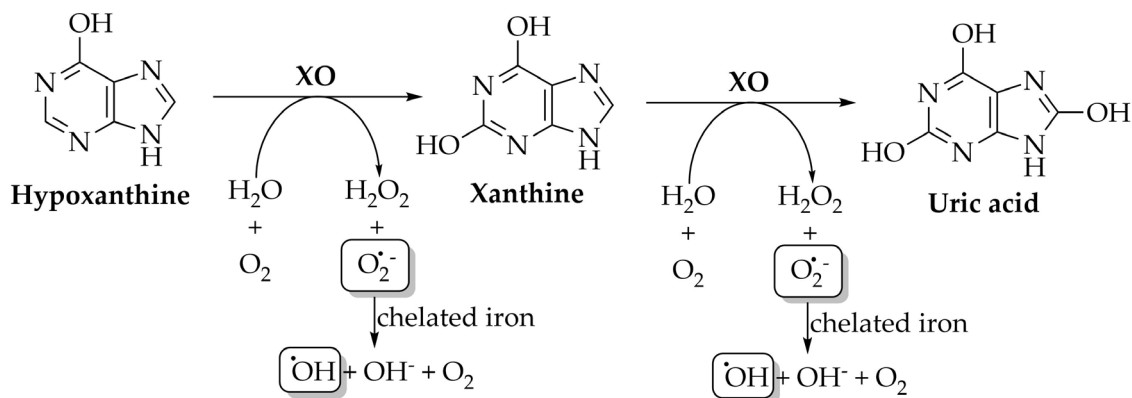


Scheme S1 – Chemical mechanism for the formation of bis-thiobarbiturate 8.

Table S1 – Full *in vitro* data for XO inhibitory activity, DPPH radical scavenging strength and cytotoxicity effects on NHDF, Caco-2 and MCF-7 cells by bis-thiobarbiturates 3-7 and 9-19 and references Febuxostat, Allo, Trolox and 5-FU.^a

Compound	XO inhibition (%)		DPPH (% scavenging at 30 μM)	Cytotoxicity (% cell viability at 30 μM)		
	30 μM	5 μM		NHDF	Caco-2	MCF-7
3	80.15 ± 0.68	10.42 ± 1.01	34.58 ± 0.96	88.65 ± 1.40	91.23 ± 9.87	89.96 ± 5.33
4	36.47 ± 2.95	-	42.64 ± 0.81	95.57 ± 7.26	98.58 ± 5.70	90.64 ± 3.92
5	86.12 ± 2.41	52.92 ± 4.02	34.76 ± 1.42	86.48 ± 5.92	62.52 ± 11.94	90.68 ± 4.06
6	92.25 ± 0.09	56.82 ± 2.16	34.99 ± 1.32	99.78 ± 5.43	100.13 ± 4.45	91.68 ± 1.48
7	20.86 ± 2.47	-	32.41 ± 0.26	96.60 ± 4.32	97.09 ± 3.63	98.66 ± 4.83
9	45.61 ± 1.69	-	39.63 ± 2.26	81.35 ± 8.87	67.49 ± 9.4	90.18 ± 5.70
10	23.53 ± 0.17	-	38.12 ± 1.56	57.11 ± 8.12	62.6 ± 7.74	100.16 ± 13.01
11	95.72 ± 1.49	80.92 ± 0.59	57.25 ± 0.98	94.27 ± 7.84	72.31 ± 9.76	92.15 ± 3.68
12	72.25 ± 5.65	-	42.92 ± 0.61	85.64 ± 7.17	90.88 ± 3.84	91.70 ± 4.91
13	89.73 ± 1.41	37.42 ± 2.55	29.90 ± 0.50	75.80 ± 2.41	95.43 ± 4.17	98.22 ± 3.25
14	90.70 ± 0.71	56.29 ± 1.21	28.04 ± 0.25	80.13 ± 7.69	97.2 ± 2.97	88.06 ± 3.25
15	14.92 ± 1.68	-	32.33 ± 0.48	91.18 ± 7.77	96.91 ± 4.73	91.25 ± 4.26
16	61.44 ± 1.22	-	31.35 ± 0.91	60.68 ± 1.72	95.36 ± 3.30	91.11 ± 2.00
17	90.75 ± 2.87	55.2 ± 1.63	40.90 ± 0.65	68.89 ± 9.33	88.72 ± 7.85	86.62 ± 5.87
18	98.85 ± 0.82	63.43 ± 2.1	31.04 ± 0.66	86.55 ± 2.38	94.68 ± 7.19	88.29 ± 3.29
19	91.68 ± 1.87	67.3 ± 1.27	3.83 ± 2.44	81.01 ± 3.57	80.71 ± 12.98	93.67 ± 5.68
Febuxostat	95.03 ± 0.91	93.88 ± 2.84	-	-	-	-
Allo	88.51 ± 3.64	26.93 ± 0.82	0.48 ± 0.21	-	-	-
Trolox	-	-	54.86 ± 0.98	-	-	-
5-FU	-	-	-	20.93 ± 0.83	37.06 ± 1.51	45.88 ± 4.72

^a Results are expressed as average values ± standard deviation (SD) of at least two independent determinations.



Scheme S2 – Diagram of XO oxidative hydroxylation of hypoxanthine over xanthine and uric acid, with reactive oxygen species (superoxide anion radical and hydroxyl radical) generation (adapted from Šmelcerović *et al.* [1¹]).

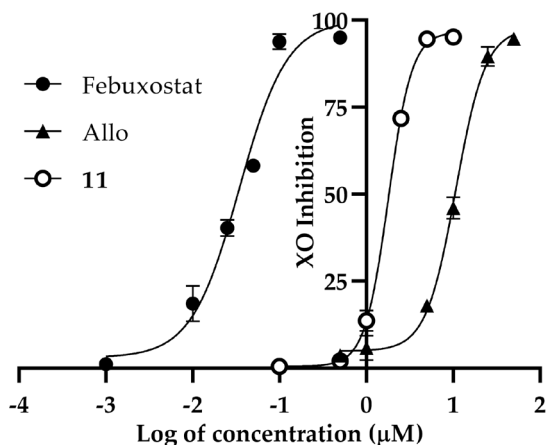


Figure S1 – IC₅₀ curves for XO inhibition by Febuxostat, Allo and bis-thiobarbiturate **11**.

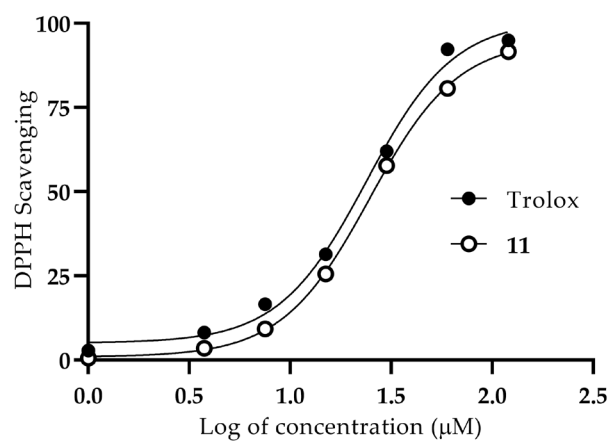


Figure S2 – IC₅₀ curves for DPPH scavenging activity of Trolox and bis-thiobarbiturate **11**.

¹ Šmelcerović, A.; Tomović, K.; Šmelcerović, Ž.; Petronijević, Ž.; Kocić, G.; Tomašić, T.; Jakopin, Ž.; Anderluh, M. Xanthine oxidase inhibitors beyond allopurinol and febuxostat; an overview and selection of potential leads based on in silico calculated physico-chemical properties, predicted pharmacokinetics and toxicity. *Eur J Med Chem* 2017, 135, 491-516.

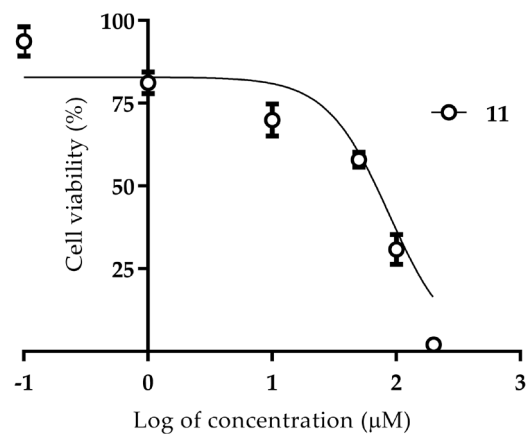


Figure S3 – IC₅₀ curve for cytotoxicity of bis-thiobarbiturate **11** on NHDF cell line.

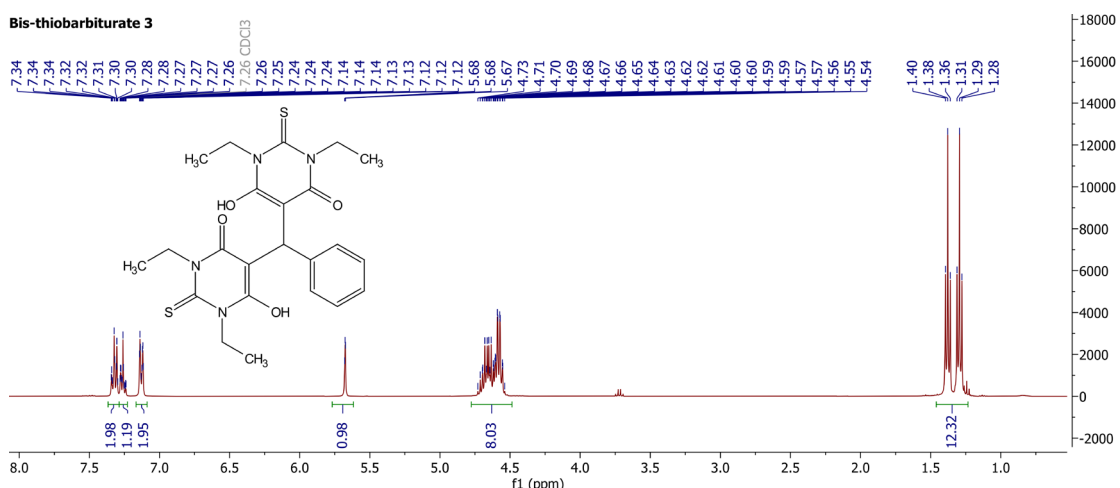


Figure S4 – ^1H NMR of bis-thiobarbiturate **3** in CDCl_3 .

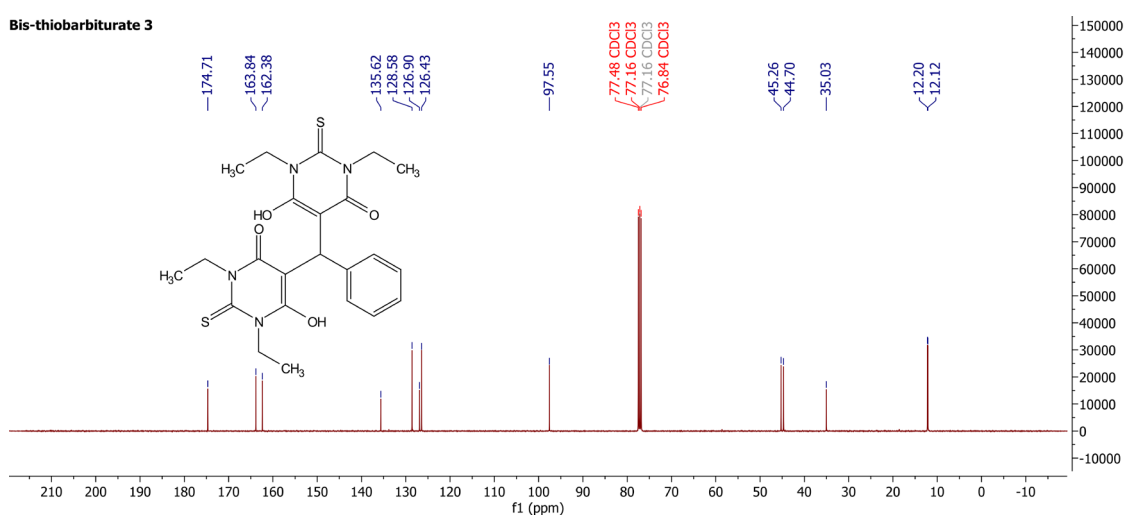


Figure S5 – ^{13}C NMR of bis-thiobarbiturate 3 in CDCl_3 .

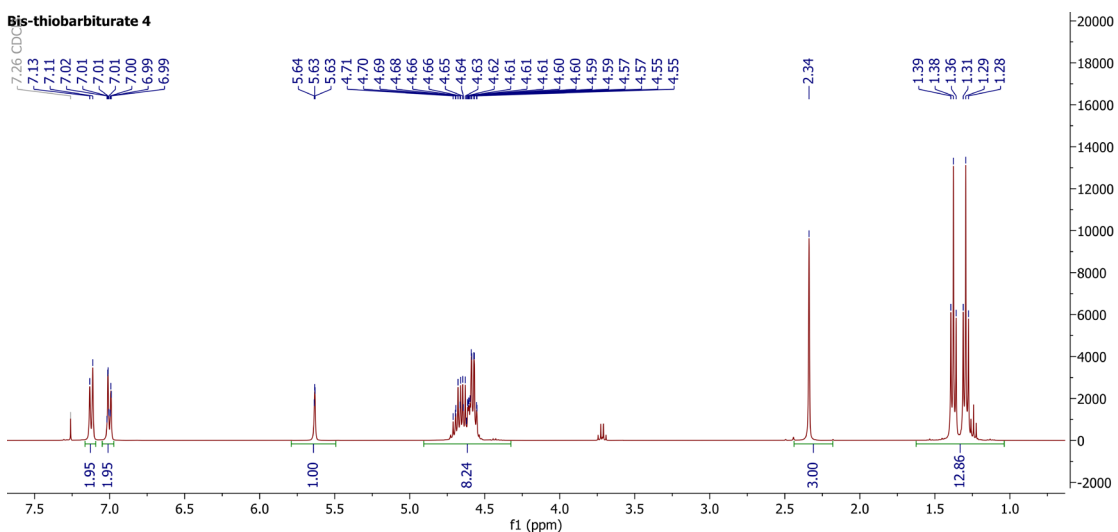


Figure S6 – ^1H NMR of bis-thiobarbiturate **4** in CDCl_3 .

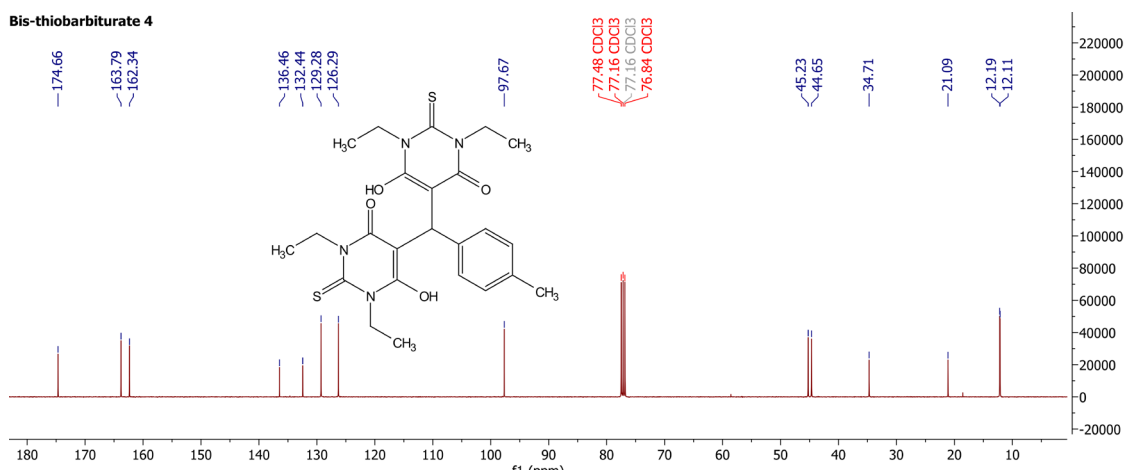


Figure S7 – ^{13}C NMR of bis-thiobarbiturate **4** in CDCl_3 .

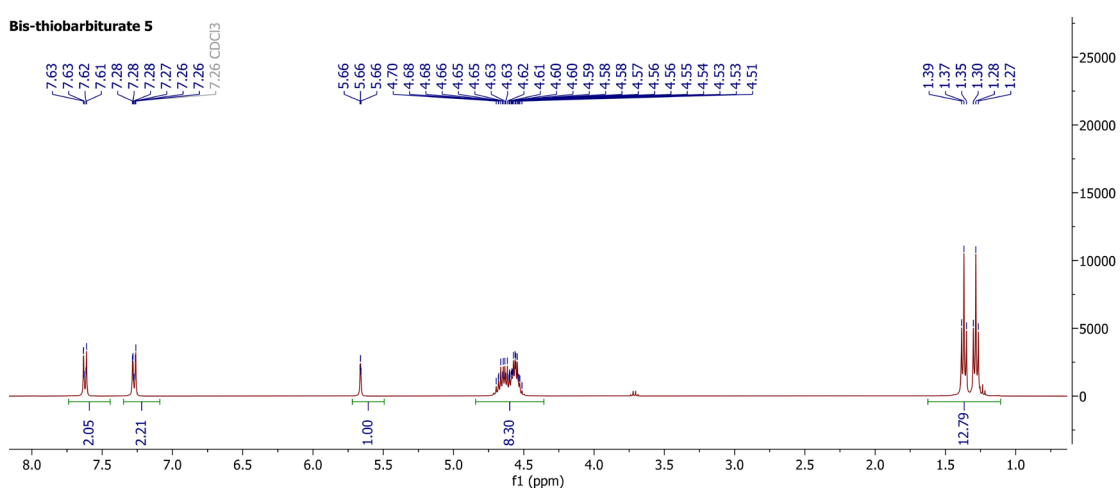


Figure S8 – ^1H NMR of bis-thiobarbiturate **5** in CDCl_3 .

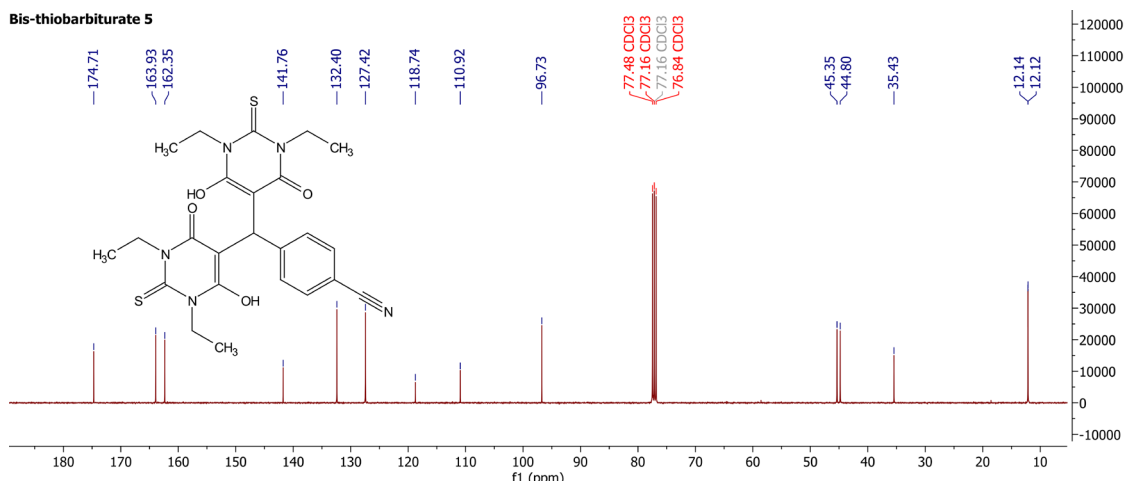


Figure S9 – ^{13}C NMR of bis-thiobarbiturate 5 in CDCl_3 .

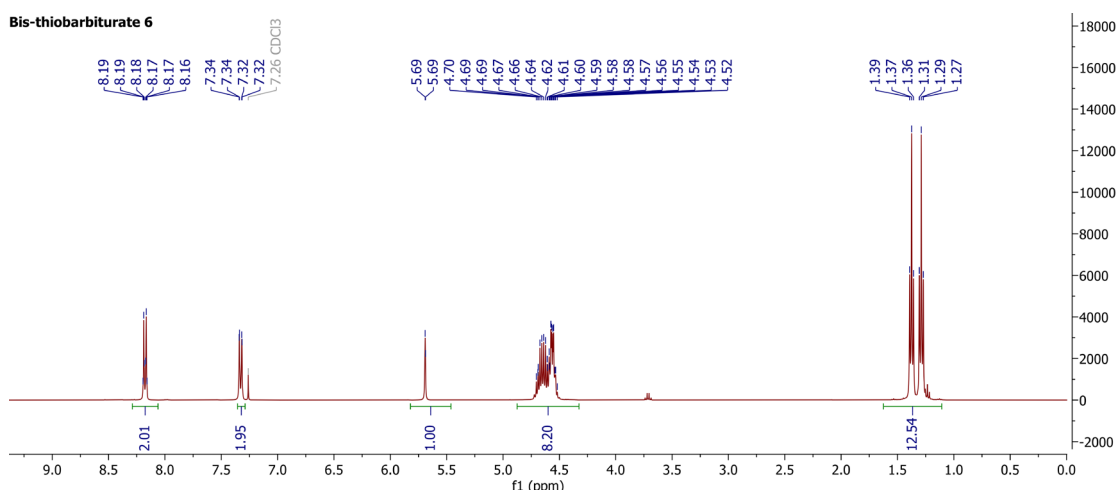


Figure S10 – ^1H NMR of bis-thiobarbiturate 6 in CDCl_3 .

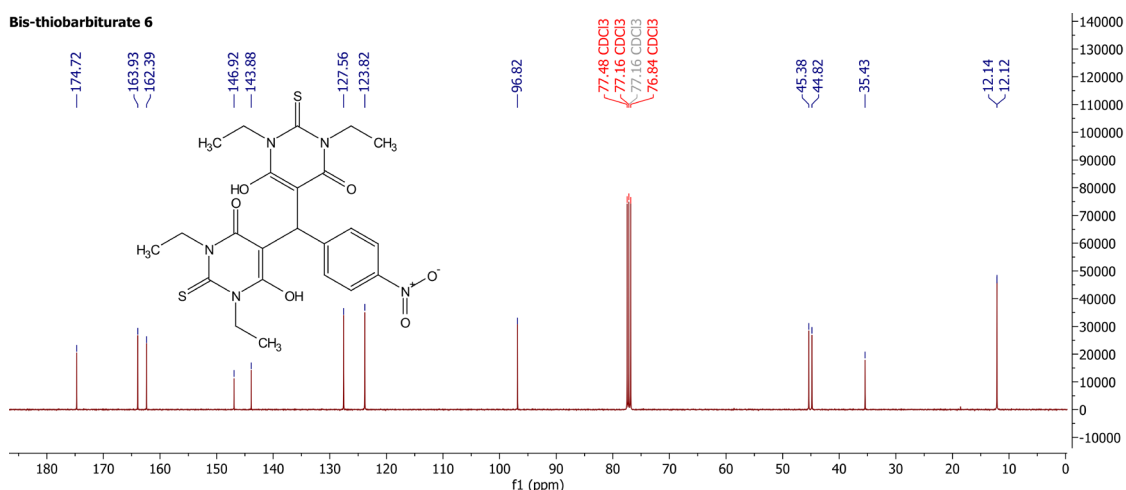


Figure S11 – ^{13}C NMR of bis-thiobarbiturate 6 in CDCl_3 .

Bis-thiobarbiturate 7

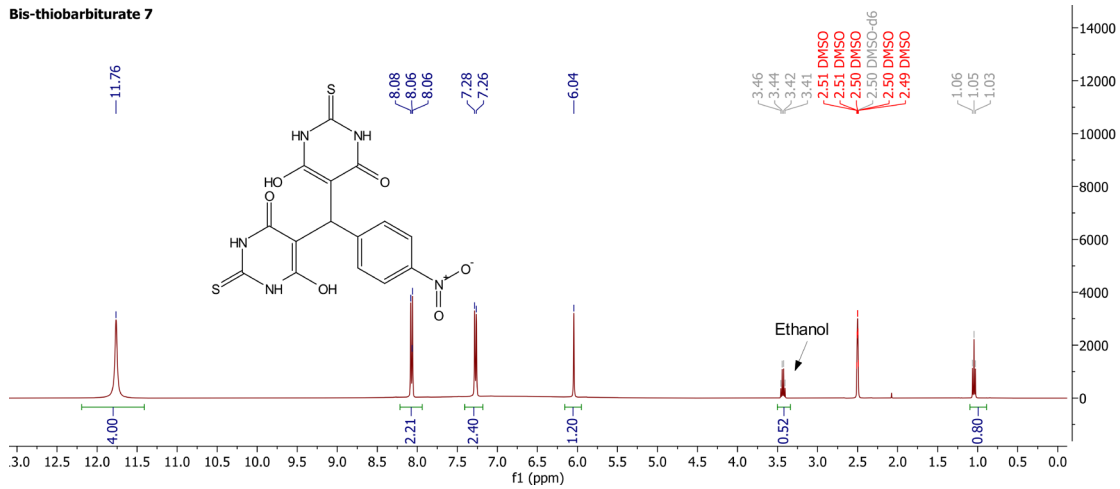


Figure S12 – ^1H NMR of bis-thiobarbiturate **7** in $\text{DMSO}-d_6$.

Bis-thiobarbiturate 7

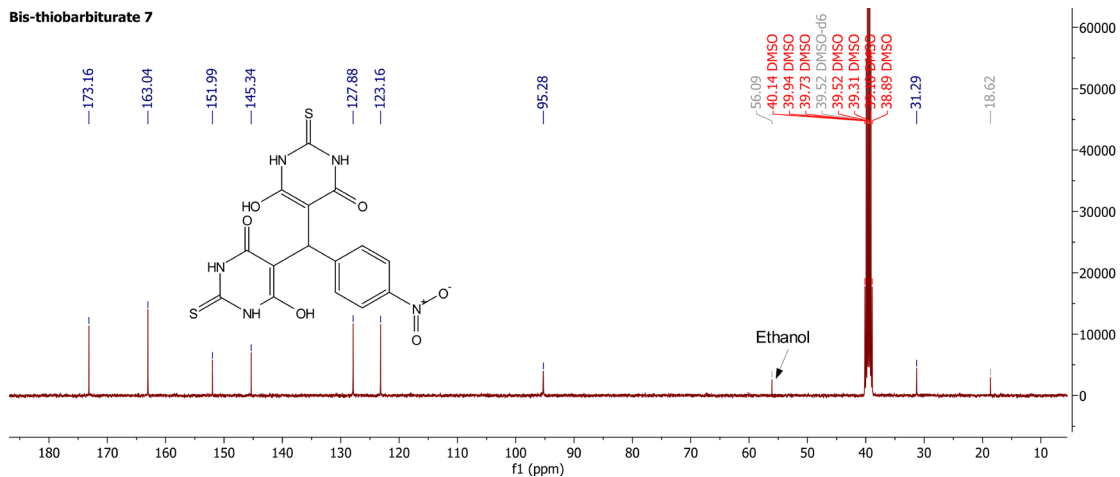


Figure S13 – ^{13}C NMR of bis-thiobarbiturate **7** in $\text{DMSO}-d_6$.

Bis-barbiturate 8

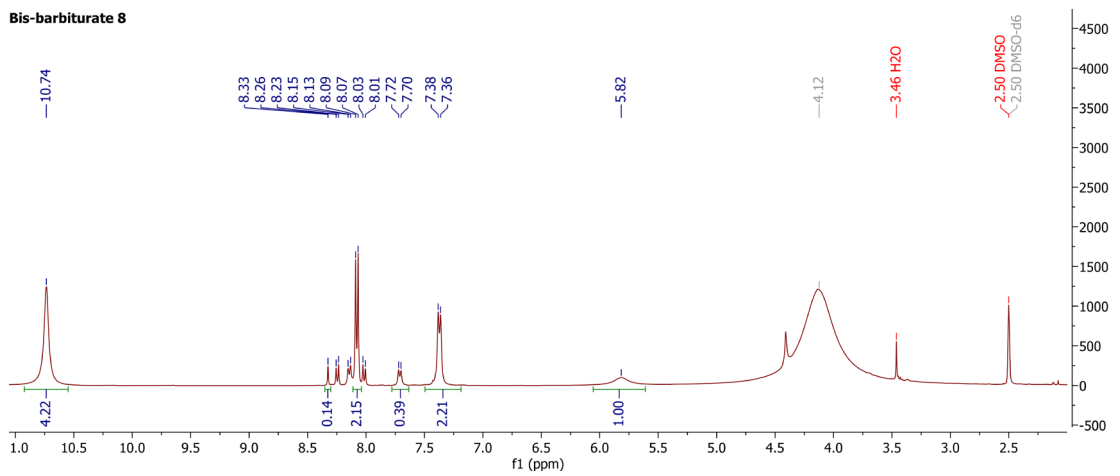


Figure S14 – ^1H NMR of bis-barbiturate 8 in $\text{DMSO}-d_6$.

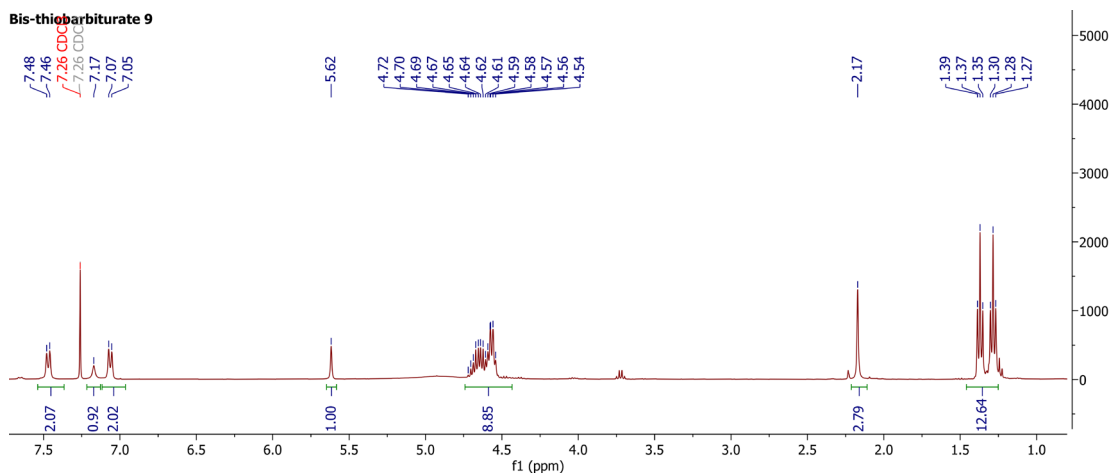


Figure S15 – ^1H NMR of bis-thiobarbiturate 9 in CDCl_3 .

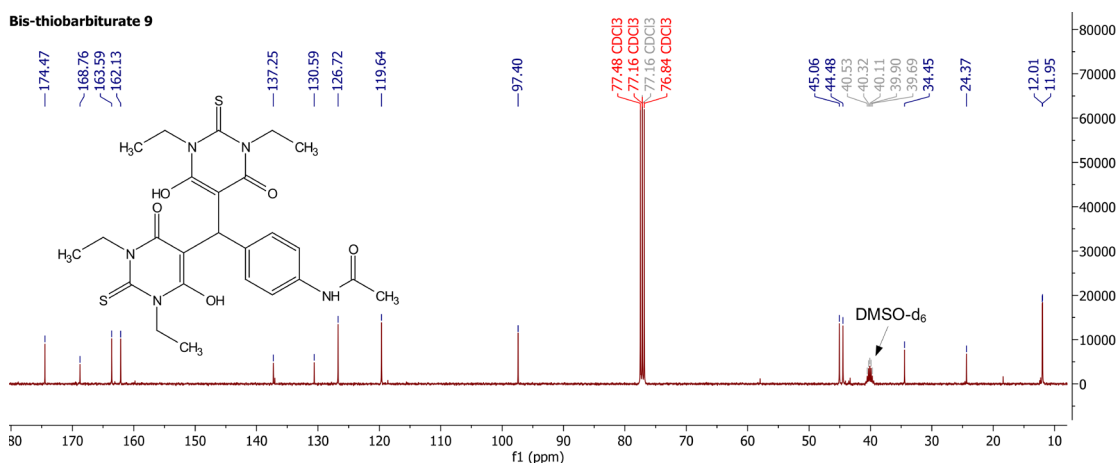


Figure S16 – ^{13}C NMR of bis-thiobarbiturate 9 in CDCl_3 .

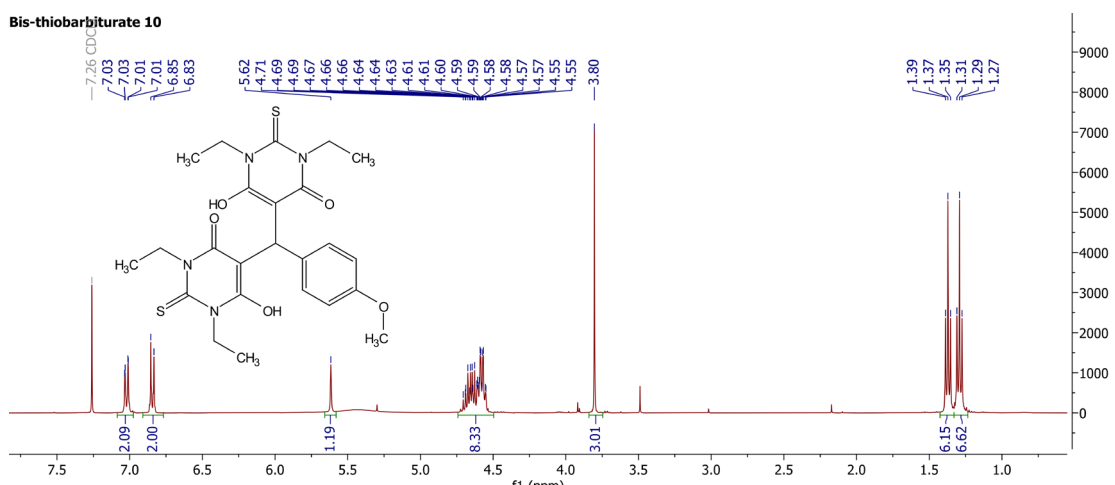


Figure S17 – ^1H NMR of bis-thiobarbiturate 10 in CDCl_3 .

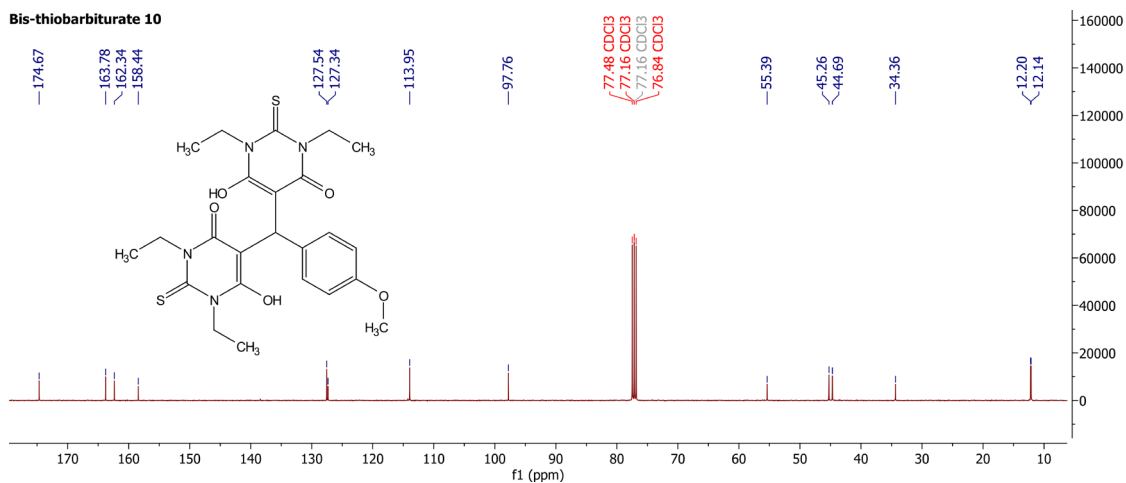


Figure S18 – ^{13}C NMR of bis-thiobarbiturate 10 in CDCl_3 .

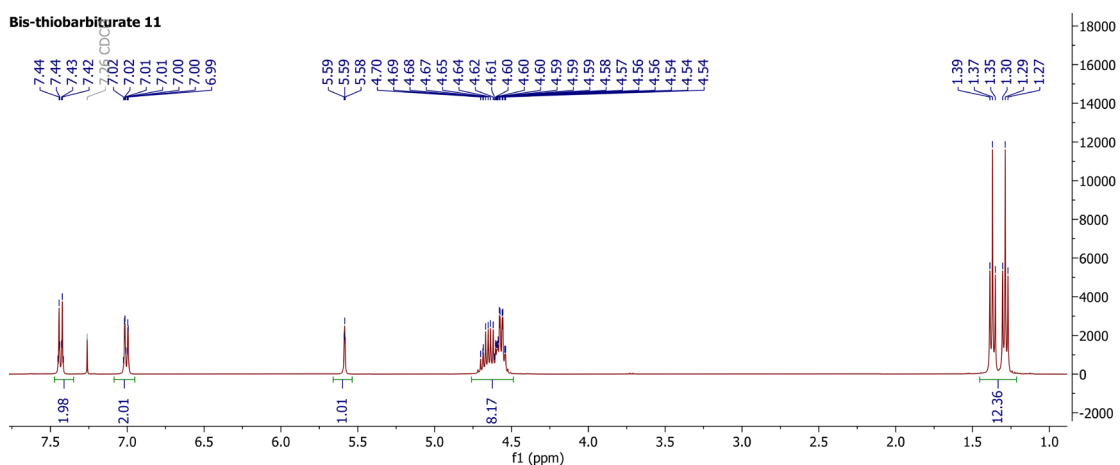


Figure S19 – ^1H NMR of bis-thiobarbiturate 11 in CDCl_3 .

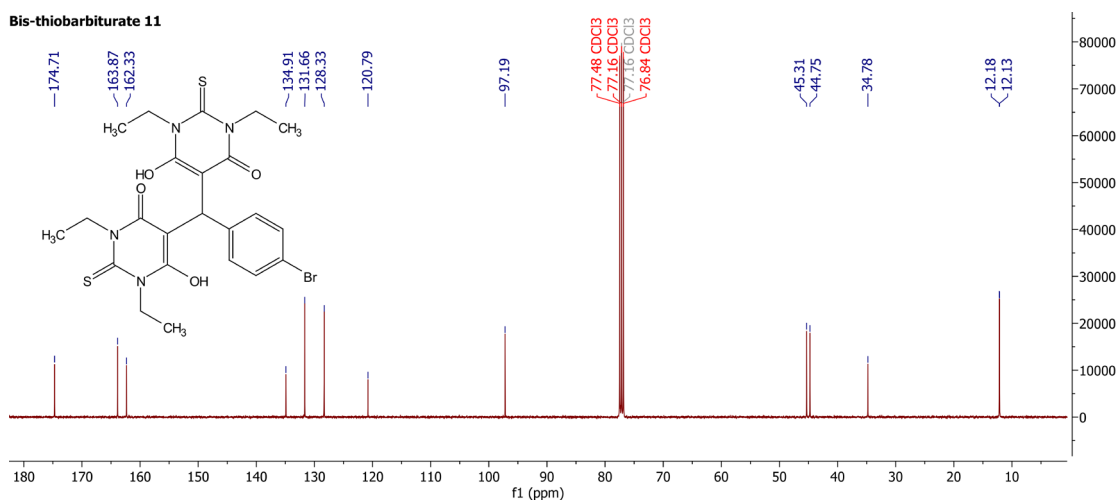


Figure S20 – ^{13}C NMR of bis-thiobarbiturate 11 in CDCl_3 .

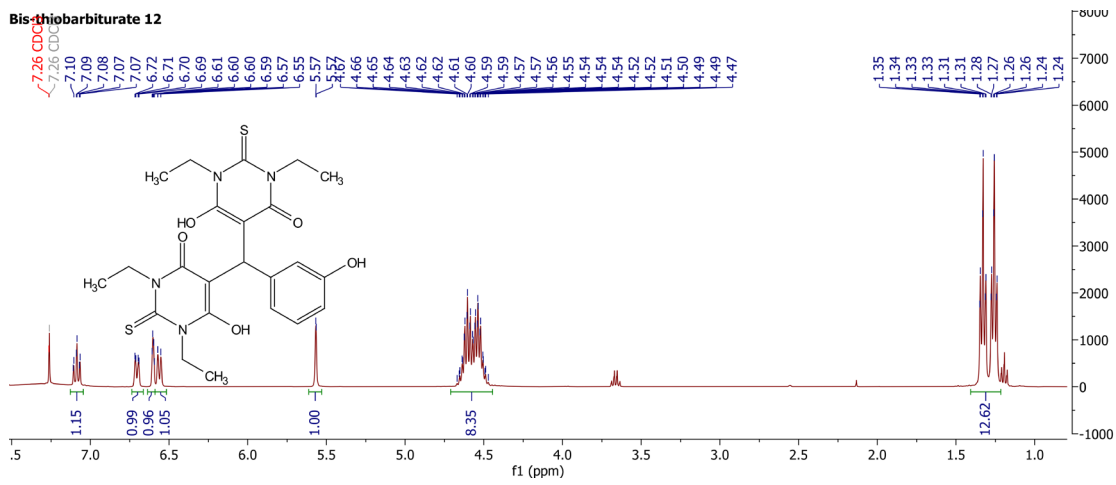


Figure S21 – ^1H NMR of bis-thiobarbiturate 12 in CDCl_3 .

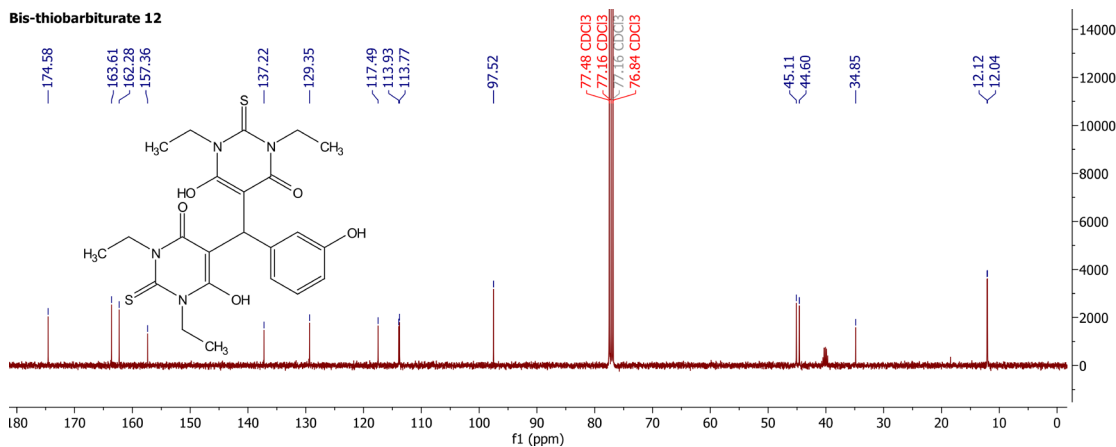


Figure S22 – ^{13}C NMR of bis-thiobarbiturate 12 in CDCl_3 .

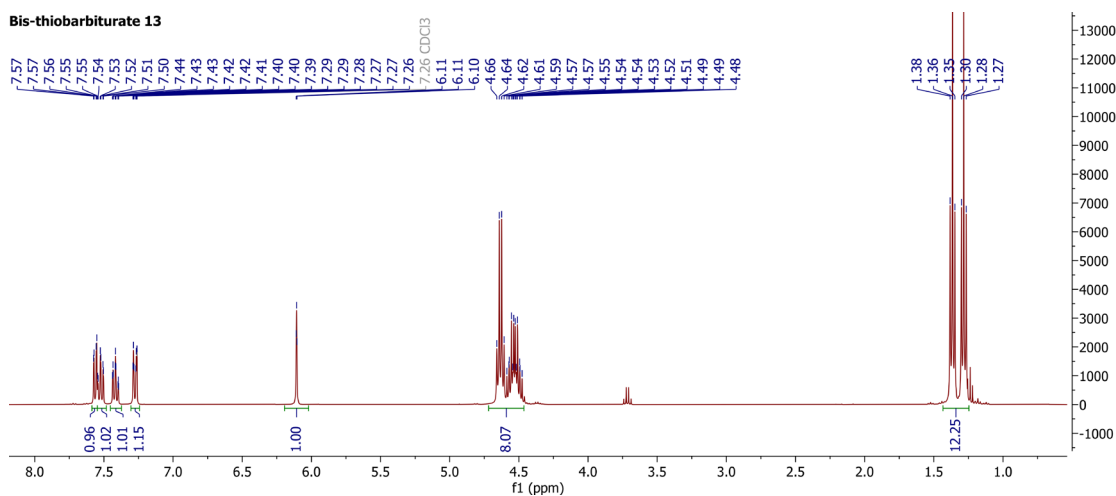


Figure S23 – ^1H NMR of bis-thiobarbiturate 13 in CDCl_3 .

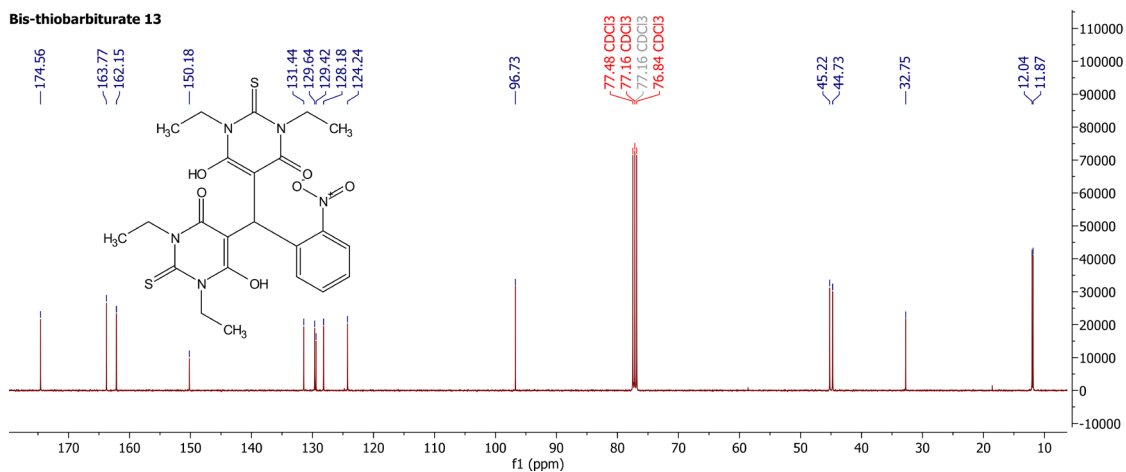


Figure S24 – ^{13}C NMR of bis-thiobarbiturate 13 in CDCl_3 .

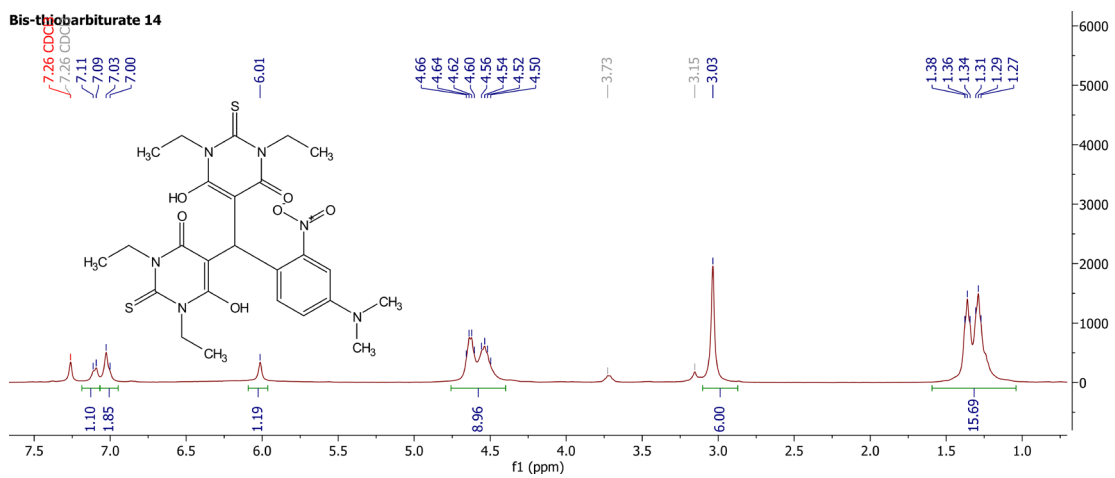


Figure S25 – ^1H NMR of bis-thiobarbiturate 14 in CDCl_3 .

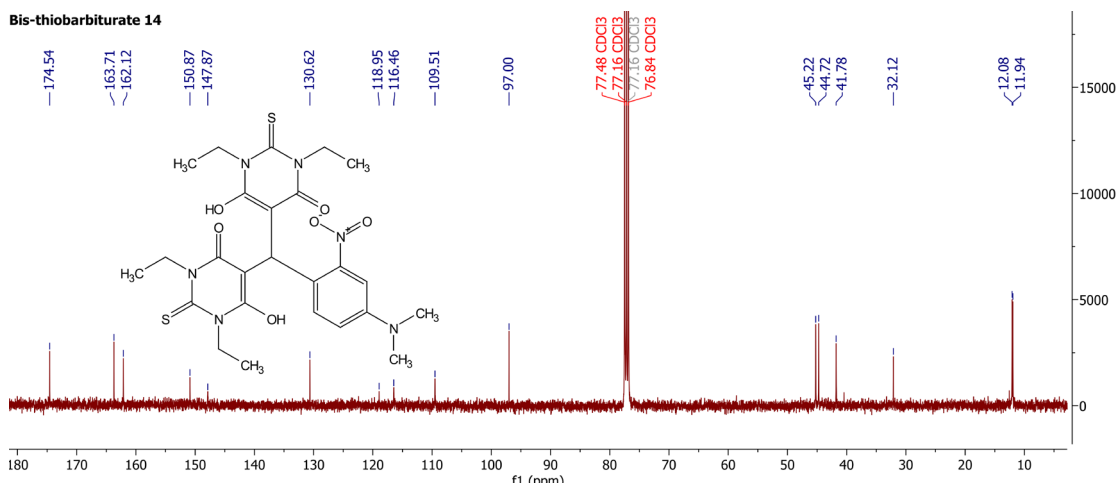


Figure S26 – ^{13}C NMR of bis-thiobarbiturate 14 in CDCl_3 .

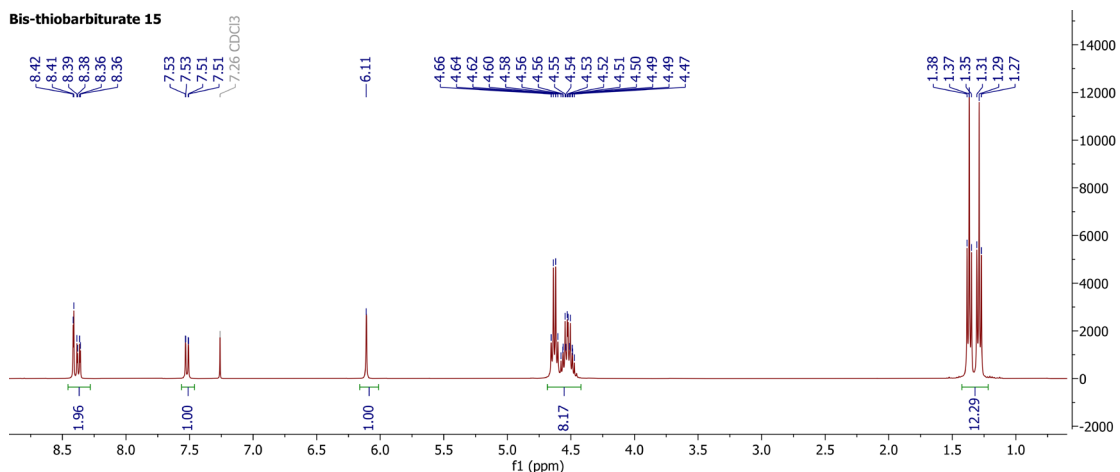


Figure S27 – ^1H NMR of bis-thiobarbiturate 15 in CDCl_3 .

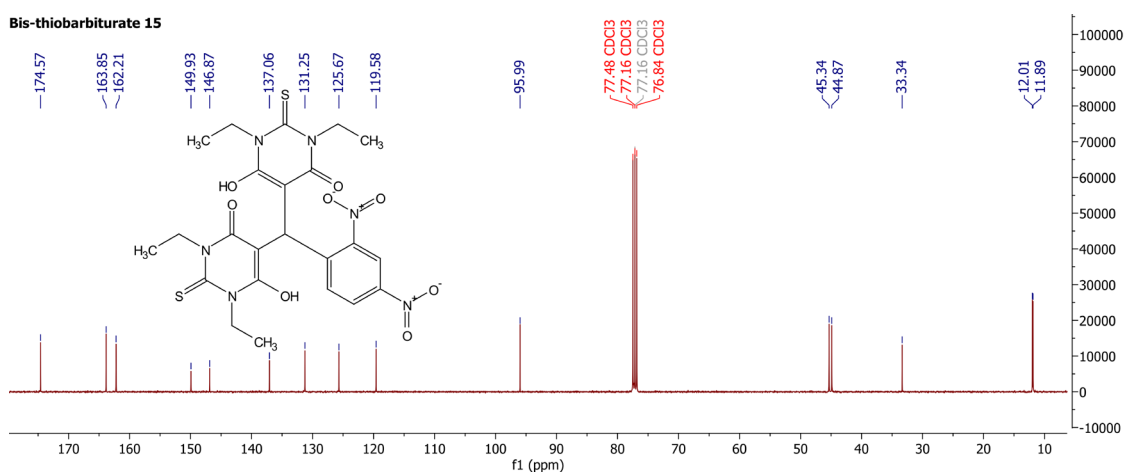


Figure S28 – ^{13}C NMR of bis-thiobarbiturate 15 in CDCl_3 .

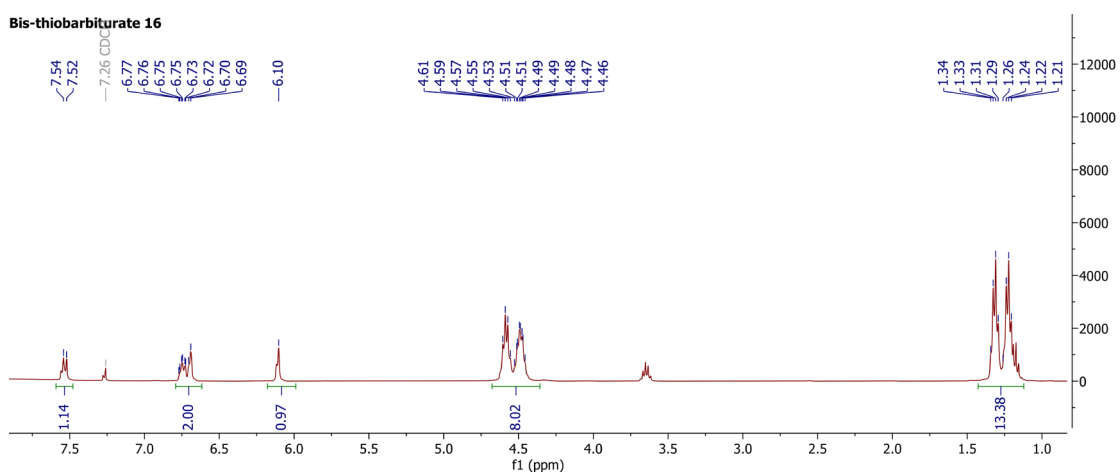


Figure S29 – ^1H NMR of bis-thiobarbiturate 16 in CDCl_3 .

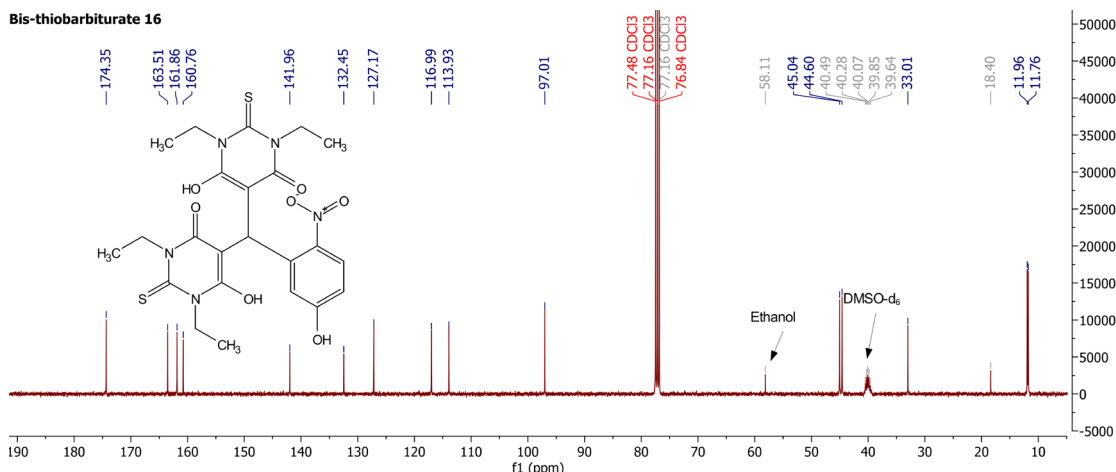


Figure S30 – ^{13}C NMR of bis-thiobarbiturate 16 in CDCl_3 .

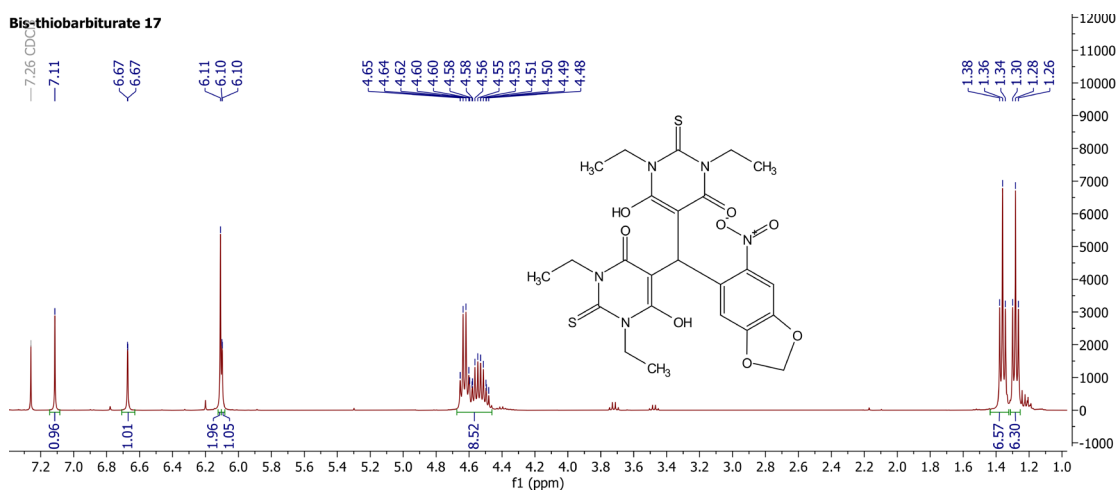


Figure S31 – ^1H NMR of bis-thiobarbiturate 17 in CDCl_3 .

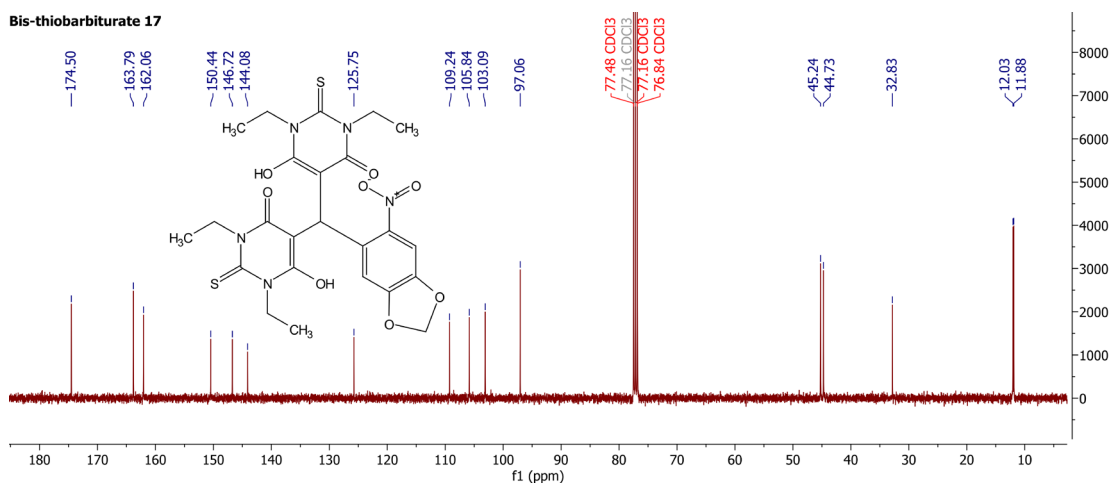


Figure S32 – ^{13}C NMR of bis-thiobarbiturate 17 in CDCl_3 .

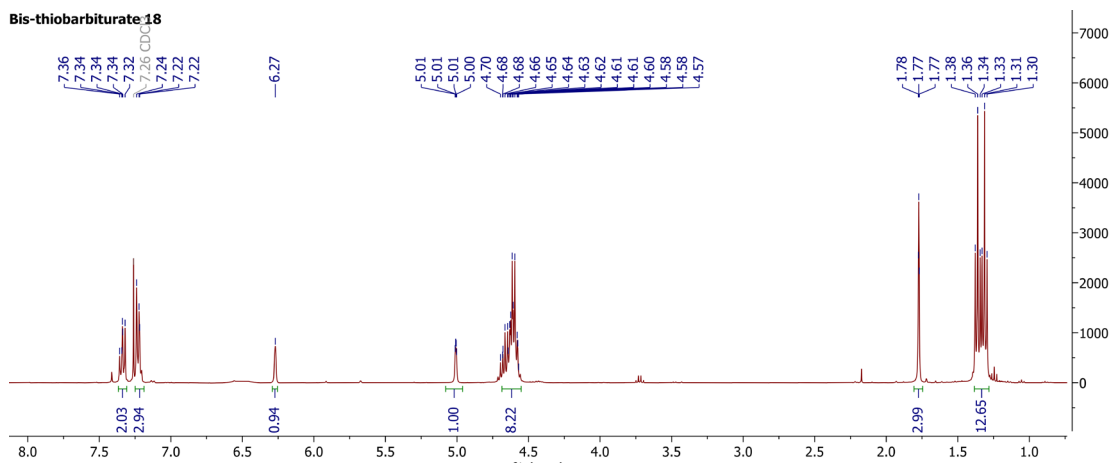


Figure S33 – ^1H NMR of bis-thiobarbiturate 18 in CDCl_3 .

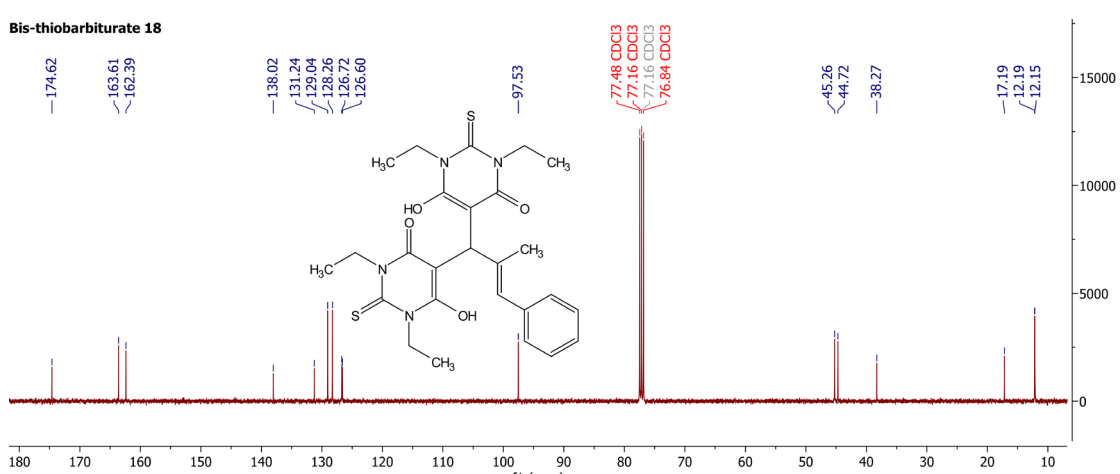


Figure S34 – ^{13}C NMR of bis-thiobarbiturate 18 in CDCl_3 .

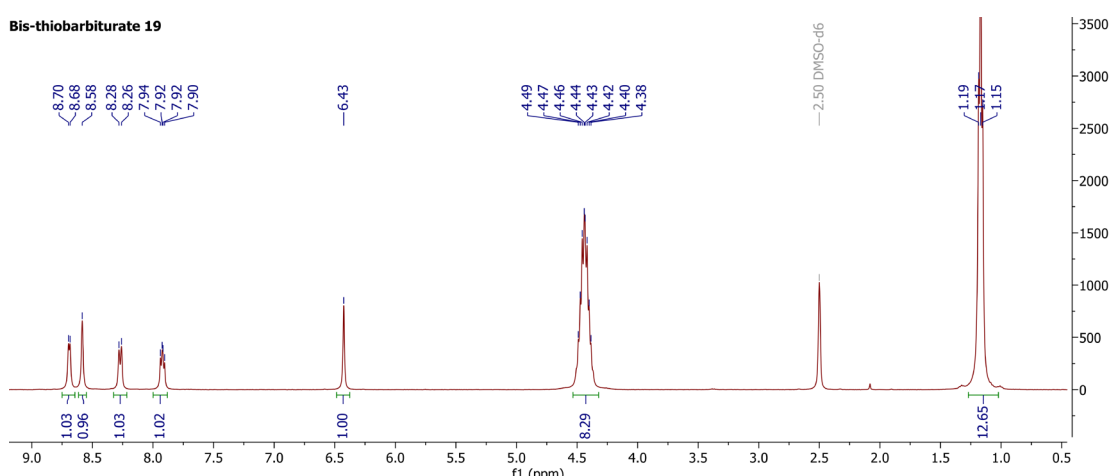


Figure S35 – ^1H NMR of bis-thiobarbiturate 19 in $\text{DMSO}-d_6$.

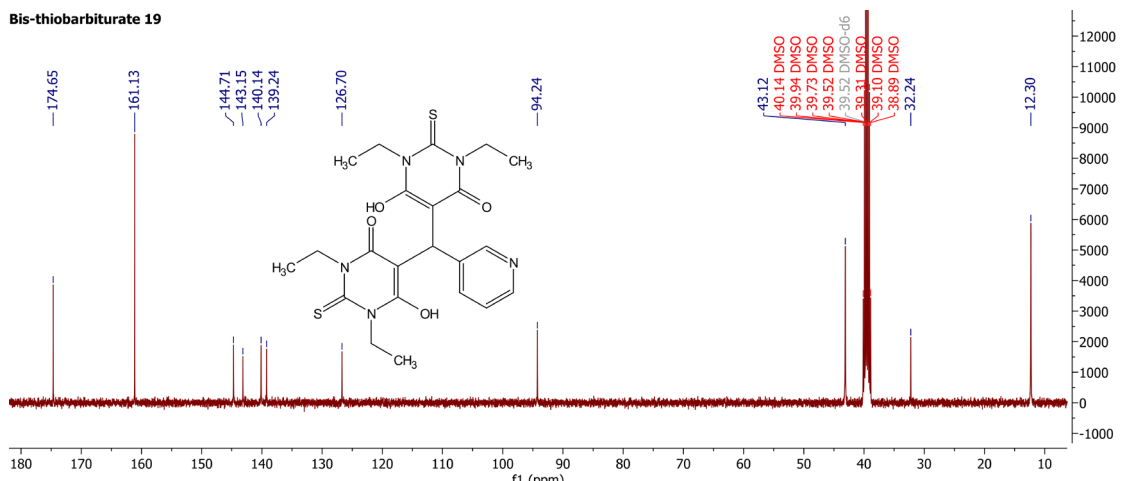


Figure S36 – ^{13}C NMR of bis-thiobarbiturate 19 in $\text{DMSO}-d_6$.